Phytomedicine 55 (2019) 179–190

Contents lists available at ScienceDirect

Phytomedicine

journal homepage: www.elsevier.com/locate/phymed

p73 induction by *Abrus* agglutinin facilitates Snail ubiquitination to inhibit epithelial to mesenchymal transition in oral cancer

Niharika Sinha[a], Biswa Ranjan Meher[b], Prajna Paramita Naik[a], Prashanta Kumar Panda[a], Subhadip Mukhapadhyay[a], Tapas K Maiti[c], Sujit K Bhutia[a,*]

[a] Department of Life Science, National Institute of Technology Rourkela, Rourkela 769008, Odisha, India
[b] Centre for Life Science, Central University of Jharkhand, Brambe, Ranchi 835205, Jharkhand, India
[c] Department of Biotechnology, Indian Institute of Technology, Kharagpur, Kharagpur 721302, India

ARTICLE INFO

Keywords:
Abrus agglutinin
Emt
Snail
P73
Erk
Ubiquitination

ABSTRACT

Background: Epithelial-to-mesenchymal transition (EMT), a key step in oral cancer progression, is associated with invasion, metastasis, and therapy resistance, thus targeting the EMT represents a critical therapeutic strategy for the treatment of oral cancer metastasis. Our previous study showed that *Abrus* agglutinin (AGG), a plant lectin, induces both intrinsic and extrinsic apoptosis to activate the tumor inhibitory mechanism.

Objective: This study aimed to investigate the role of AGG in modulating invasiveness and stemness through EMT inhibition for the development of antineoplastic agents against oral cancer.

Methods: The EMT- and stemness-related proteins were studied in oral cancer cells using Western blot analysis and fluorescence microscopy. The potential mechanisms of Snail downregulation through p73 activation in FaDu cells were evaluated using Western blot analysis, immunoprecipitation, confocal microscopy, and molecular docking analysis. Immunohistochemical staining of the tumor samples of AGG-treated FaDu-xenografted nude mice was performed.

Results: At the molecular level, AGG-induced p73 suppressed Snail expression, leading to EMT inhibition in FaDu cells. Notably, AGG promoted the translocation of Snail from the nucleus to the cytoplasm in FaDu cells and triggered its degradation through ubiquitination. In this setting, AGG inhibited the interaction between Snail and p73 in FaDu cells, resulting in p73 activation and EMT inhibition. Moreover, in epidermal growth factor (EGF)-stimulated FaDu cells, AGG abolished the upregulation of extracellular signal-regulated kinase (ERK)1/2 that plays a pivotal role in the upregulation of Snail to regulate the EMT phenotypes. In immunohistochemistry analysis, FaDu xenografts from AGG-treated mice showed decreased expression of Snail, SOX2, and vimentin and increased expression of p73 and E-cadherin compared with the control group, confirming EMT inhibition as part of its anticancer efficacy against oral cancer.

Conclusion: In summary, AGG stimulates p73 in restricting EGF-induced EMT, invasiveness, and stemness by inhibiting the ERK/Snail pathway to facilitate the development of alternative therapeutics for oral cancer.

Introduction

Oral cancer, mostly squamous cell carcinoma (SCC), is a leading cause of cancer-related death in India because of the high consumption of tobacco products, including *gutkha* and *paan* (betle) in young and middle-aged men. Moreover, it is one of the severe human cancers because of its aggressiveness, which has not changed considerably during the last three decades with the advances in the current therapies (Sinha et al., 2013; Naik et al., 2016). Interestingly, the oral SCC is associated with a high rate of invasiveness and lymph node metastasis, affecting the prognosis of the patients. During tumor metastasis, tumor cells acquire invasive property by activating the epithelial-to-mesenchymal transition (EMT) program to undergo phenotypic alternation for evading primary tumor, which is associated with invasion, metastasis, and therapy resistance (Smith et al., 2013; Cao et al., 2016; Zhang et al., 2014). For example, epidermal growth factor (EGF)-stimulated

Abbreviations: OSCC, oral squamous cell carcinoma; HNSCC, head and neck squamous cell carcinoma; SCC, squamous cell carcinoma; AGG, abrus agglutinin; EMT, epithelial-to-mesenchymal transition; RIP, ribosome inactivating protein; EGF, epidermal growth factor; ERK (1/2), extracellular signal-regulated kinase (1/2); DAPI, 4,6-diamidino-2-phenylindole dihydrochloride; DMSO, Dimethylsulfoxide; PDB, Protein Data Bank; HE, Haematoxylin eosin; H-score, Histoscore

* Corresponding author.
E-mail address: sujitb@nitrkl.ac.in (S.K. Bhutia).

https://doi.org/10.1016/j.phymed.2018.08.003
Received 28 February 2018; Received in revised form 21 May 2018; Accepted 5 August 2018

SCC cells showing increased motility, migration, invasion, metastasis, and resistance to apoptosis *in vitro* along with the downregulation of E-cadherin and upregulation of N-cadherin and vimentin (Zhu et al., 2012). Furthermore, the EMT process is controlled by a group of transcriptional factors, zinc finger proteins, and basic helix-loop-helix factors. Out of the three family members of Snail, Snail1, Snail2/Slug, and Snail3/Smuc, we studied Snail1 or Snail, as it is more commonly known. The Snail transcription factor with C2H2 zinc finger domain is a master regulator of EMT in several tumor progressions. Snail induces EMT by potentially binding to the E-box consensus sequence of epithelial gene E-cadherin, leading to its transcriptional repression, followed by decreased cell adhesion to the neighboring cells (Smith et al., 2013; Zhang et al., 2014; Baulida et al., 2015; Naik et al., 2016).

Snail interacts with p53 family proteins to regulate EMT, invasion, and metastasis (Powell et al., 2014; Chang et al., 2011). Furthermore, its degradation is facilitated by the ability of p53 to bind to it, followed by MDM2-mediated ubiquitination (Lee et al., 2009; Lim et al., 2010). In addition, inhibiting the direct binding between Snail and the DNA-binding domain of p53 resulted in the restoration of p53 expression in K-Ras-mutated cancers, including pancreatic, lung, and colon cancers. In mammalian neural precursors, Snail enhanced cell survival by antagonizing a p53-dependent death pathway, as the coincident p53 knockdown rescues survival deficits caused by Snail knockdown. P53 knockdown rescued cells by altering cell death and/or proliferation (Zander et al., 2014). Another member of the p53 family, p73 or TAp73, suppressed EMT with an increased E-cadherin expression and decreased EMT transcription factors (Thakur et al., 2016), but DNp73 enhanced Slug upregulation and facilitated an EMT-like phenotype with the loss of E-cadherin (Steder et al., 2013). Interestingly, TAp73 knockdown and its downstream targets p21 and PUMA increased the EMT transcriptional factors with a decrease in E-cadherin in Madin-Darby canine kidney cell, confirming the critical role of p73 in EMT regulation (Zhang et al., 2015). The detail role of p73 proteins in EMT, cancer cell stemness, and invasion through Snail in oral cancer has not been elucidated.

Genetic alterations resulting in the mesenchymal phenotypic change in cancer cells lead to activation of either of the two prosurvival pathways PI3K/Akt and MEK–1/2/extracellular signal-regulated kinase (ERK)1/2 to establish in the metastatic sites (Gkouveris et al., 2014; Smith et al., 2014). In addition, activated Raf/MEK/ERK, MSK1, Elk–1, and Snail lead to the downregulation of E-cadherin in different types of cancer, including breast cancer (Smith et al., 2014). Furthermore, chemokine (C-X-C) ligand 5 may activate Raf/MEK/ERK, MSK1, Elk–1, and Snail, leading to the downregulation of E-cadherin. Interestingly, it was observed that Snail and ERK(1/2) were regulated by each other to induce EMT in MCF–7 cells. Moreover, the overexpression of ERK/MAP kinases was reported in different grades of SCC in patients with oral cancer, indicating its candidature as a potential therapeutic target in oral cancer (Mishima et al., 1998). Although differential p73 isoform exists (Fernandez-Alonso et al., 2015), p73 induces sustained activation of ERK signaling cascade in association with oncogenic Ras in the absence of p53 for cellular outcome and differentiation (Fernandez-Garcia et al., 2007). A recent study showed that the p73-dependent activation of ERK promotes metastasis in proapoptotic stress response factor TP53INP1 deficient conditions in hepatocellular carcinoma cells (Ng et al., 2017).

Abrus agglutinin (AGG) is a low-toxicity, heterodimeric, galactose-specific lectin isolated from the seeds of *Abrus precatorius* having two A chains and B chains linked by a disulfide bond. In addition, it belongs to the ribosome-inactivating protein family II and inhibits protein synthesis through the rRNA *N*-glycosidase activity of A chain after cellular internalization (Hegde et al., 1991). AGG displays ubiquitous antitumor activity through multiple cellular targeting in different cancer types (Ghosh and Maiti, 2007; Mukhopadhyay et al., 2014; Bhutia et al., 2008a, b; Behera et al., 2014a, b). We and other showed that AGG induces both intrinsic and extrinsic apoptosis through the Akt-ROS-dependent pathway to activate tumor inhibitory mechanism (Bhutia et al., 2016). Moreover, AGG inhibits angiogenesis by targeting proangiogenic factor IGFBP–2 signaling pathway (Bhutia et al., 2016). Interestingly, AGG inhibits Akt/PH domain to stimulate autophagic cell death through the induction of endoplasmic reticulum stress in cervical cancer (Panda et al., 2017). Our previous study showed that AGG prevents tumor growth and causes irreparable DNA damage to induce apoptosis through ROS-mediated ATM-p73-dependent pathway in oral cancer (Sinha et al., 2017a). Furthermore, it showed that AGG inhibits the growth of cancer stem cells (CSCs) derived from FaDu cells by inactivating Wnt/β-catenin signaling pathway (Sinha et al., 2017b). In this study, we established the detail role of AGG in modulating EMT and stemness through the p73-dependent pathway. Interestingly, AGG encourages p73 in governing EGF-induced EMT, invasion, and stemness by inhibiting the ERK/Snail pathway to facilitate the development of alternative therapeutics for oral cancer.

Material and methods

Chemical and reagents

4,6-Diamidino-2-phenylindole dihydrochloride (DAPI) and dimethylsulfoxide were purchased from Sigma-Aldrich (St. Louis, MO, USA). Fetal bovine serum (sterile filtered, South American origin), minimal essential medium (MEM), trypsin, antibiotic-antimycotic solution, and Lipofectamine 2000 were purchased from Invitrogen (Carlsbad, CA, USA). Antibodies against E-cadherin, p73, N-cadherin, vimentin, SOX2, OCT4, nestin, EGFR and actin, EGF, and Boyden chamber were purchased from BD Biosciences, San Jose, CA, USA. Involucrin (Santa Cruz Biotechnology, Dallas, TX, USA), ADAM17 (Abcam, Cambridge, MA, USA), Snail and PD98059 (Cell Signaling Technology, Danvers, MA, USA), and MG–132 (Calbiochem, San Diego, CA, USA) were procured. Plasmids used were obtained from Addgene (Cambridge, MA 02139, USA): p73DD (#22978), Snail (plasmid #16218), and an empty backbone pcDNA3 plasmid (#10792).

Abrus agglutinin purification

AGG was isolated and purified from *Abrus precatorius* seeds using ammonium sulfate fractionation, followed by lactamyl sepharose affinity chromatography and Sephadex G–100 gel permeation chromatography. The activity of isolated AGG was measured by hemagglutination assay, and the protein purity was subsequently analyzed by SDS-PAGE, native-PAGE, and gel permeation by HPLC (Hedge et al., 1991).

Cell culture

FaDu (hypopharyngeal SCC) cell line was cultured in MEM, CAL 27 and immortalized primary human fetal astrocyte (IM-PHFA) in DMEM, supplemented with antibiotic-antimycotic (1 X) and 10% fetal bovine serum.

Immunofluorescence

After EGF (20 ng/m) stimulation for 1 h, FaDu cells were treated with AGG for 24 h, followed by fixation, permeabilization, and overnight incubation of primary antibodies (1:100; E-cadherin, involucrin, N-cadherin, vimentin, β-catenin, and p73). The cells were further incubated with the secondary anti-rabbit and/or anti-mouse antibodies conjugated with Alexa Fluor to study the fluorescence of the desired proteins. Imaging was performed at a 40× fluorescence microscope (Olympus IX71; Panda et al., 2017).

Cell viability by MTT assay

About 1×10^4 IM-PHFA cells/well were cultured in a 96-well plate

at 37 °C, and treated with different concentrations of AGG for 24 h. All experiments were performed in triplicate and the relative cell viability was expressed as the percentage relative to the untreated control cells.

Confocal microscopy study

EGF (20 ng)-induced FaDu cells were grown on chamber slides for 24 h. Cells were treated with AGG for 24 h and then fixed in 10% formaldehyde, washed with phosphate buffered saline (PBS), and permeabilized with 0.2% Triton X–100 for 20 min at room temperature, followed by overnight incubation with Snail antibody. Cells were then washed with PBS and incubated with secondary antibody for 6 h, followed by DAPI counterstaining. Cell images were captured at 630× magnification using a confocal microscope (Leica TCS SP8, Wetzlar, Germany) at 561/405 nm laser wavelengths to detect Snail (red) and DAPI (blue) emissions, respectively (Panda et al., 2017).

Cell invasion assay

FaDu cells were seeded in the upper compartment of the Transwell insert containing matrigel with a pore size of 8 μm (5000 cells/) in the serum-free culture medium. Medium with 10% fetal bovine serum was added to the lower chamber as a chemoattractant factor. After a 24-h treatment with AGG, the noninvading cells on the upper surface of the membrane were gently removed with a cotton swab and fixed with 4% methanol and stained with hematoxylin and eosin for 10 min. The fixed cells were then observed under a bright field microscope at 10× bright field, and the number of cells was counted per visual fields (Bhutia et al., 2016).

Western blotting and immunoprecipitation analysis

FaDu cells were treated with AGG, followed by protein extraction. Cell extracts were prepared in cell lysis buffer, an equal amount of proteins was resolved by SDS-PAGE and transferred to PVDF membranes, and the protein levels were evaluated using antibody against E-cadherin, N-cadherin, involucrin, vimentin, β-catenin, SOX2, OCT4, nestin, p73, Snail, ERK, EGRP, and ADM17 as described previously (Sinha et al., 2017a). For immunoprecipitation analysis, cell lysates were incubated overnight at 4 °C with anti-p73 and anti-Snail antibodies, followed by coupling with protein A-Sepharose and Western blotting as described elsewhere (Sinha et al., 2017a).

Modeling p73-Snail complex through docking and molecular dynamics simulation

The crystal structures of tumor protein p73 and Snail protein were obtained from the Protein Data Bank (PDB). The PDB entries were 3VD1 and 3W5K. The X-ray structures of the p73 domain were missing some residues and atoms from 103–114, which were eventually predicted by I-TASSER software. The p73 domain contains 636 residues after modeling through I-TASSER. Because of the unavailability of a complete crystal structure of Snail protein, I-TASSER software predicted its three-dimensional structure. The Snail domain contains 264 residues after modeling through I-TASSER. The docking algorithm was then used to locate the optimal configuration of the Snail protein close to the active site of p73. Initially, the Snail domain was positioned near the active site, and the docking algorithm was performed by the ClusPro 2.0 protein-protein docking server (Comeau et al., 2004). Using the protein-protein docking algorithms, the optimal orientation of two proteins can be found by scoring the energy based on the van der Waals interactions and corresponding electrostatics. Therefore, the grid-based score was generated by calculating the non-bonded terms of the molecular mechanics force field, and the structure with the highest score was then considered for the molecular dynamics (MD) simulation (Panda et al., 2017).

Plasmids and transfections

FaDu cells were transfected according to the manufacturer's instructions. The transfections were performed in the presence of p73DD (Addgene plasmid # 22978), Snail (Plasmid # 16218), and an empty backbone pcDNA3 plasmid (Addgene plasmid # 10792), which was used for mock transfection. After 48 h of transfection, the cells were stimulated with EGF (20 ng/ml) for 1 h and used to study the expression of the target protein.

Immunohistochemical staining and scoring

For evaluating the immunohistochemical results, formalin-fixed and paraffin-embedded specimens of 3 to 4 μm thickness were sectioned and staining was performed using antiCD44 (BD Biosciences, India) and β-catenin (BD Biosciences, India) as described previously (Sinha et al., 2017a). The semiquantitative immunohistochemical score or histoscore (H-score) was obtained using a modified scoring method. The percentage of positive cells in each high power field (400× magnification) was calculated and assigned a relative staining intensity score of 1, 2, or 3 for low, intermediate, and high staining, respectively. The H-score was finally calculated as the product of the percentage of positive cells and staining intensity for each primary antibody using the formula (1 × percentage of cells staining weakly positive) + (2 × percentage of cells staining moderately positive) + (3 × percentage of cells staining strongly positive). The H-score ranges from 0 to 300 for each high power field.

Statistical analysis

All data were representative of at least five independent experiments, which were quantified and plotted as mean ± standard deviation. Student's *t*-test was used for evaluating statistical differences between experimental groups. Furthermore, nonparametric tests for statistical analysis among groups were performed by one-way analysis of variance and Kruskal-Wallis test, with Dunn's multiple group comparison tests as appropriate. Statistical analyses were performed using the SPSS Statistics 20 (IBM SPSS software, version: 20.0, Chicago, IL, USA) and GraphPad Prism 5 (GraphPad Software, Inc., San Diego, CA, USA). The *p*value was defined as follows: not significant: $p > 0.05$; $^{*}p < 0.05$; $^{**}p < 0.01$ was considered statistically significant.

Results

Abrus agglutinin inhibits epithelial-to-mesenchymal transition and stemness in oral cancer

The EMT program disrupts the epithelial sheet and gains mesenchymal phenotype with enhanced cell motility and is associated with cell migration, invasion, and stemness (Smith et al., 2013; Naik et al., 2016). To examine whether AGG inhibits EMT in oral cancer, we aimed to determine the expression of different EMT markers upon AGG treatment in FaDu and CAL 27 cells. This study data showed that AGG can upregulate the expression of epithelial markers E-cadherin and involucrin, and downregulate the expression of mesenchymal markers N-cadherin and vimentin (Fig. 1A-D) as demonstrated by immunofluorescence and Western blot analysis. Moreover, mesenchymal cells exhibit CSC-like feature with the self-renewal property that maintains the population of tumorigenic cells. Notably, AGG effectively suppresses the aberrant cytoplasmic expression of β-catenin as observed in the immunofluorescence study (Fig. 1A-D). Furthermore, the Western blotting analysis showed that AGG restricted the expression of SOX2, OCT4, and nestin that support the plasticity of CSCs (Fig. 1D). Our previous study showed that AGG inhibited activation glycogen synthase kinase 3 β in orospheres derived from FaDu cells (Sinha et al., 2017b). Moreover, our data showed that AGG did not show any cytotoxic effect

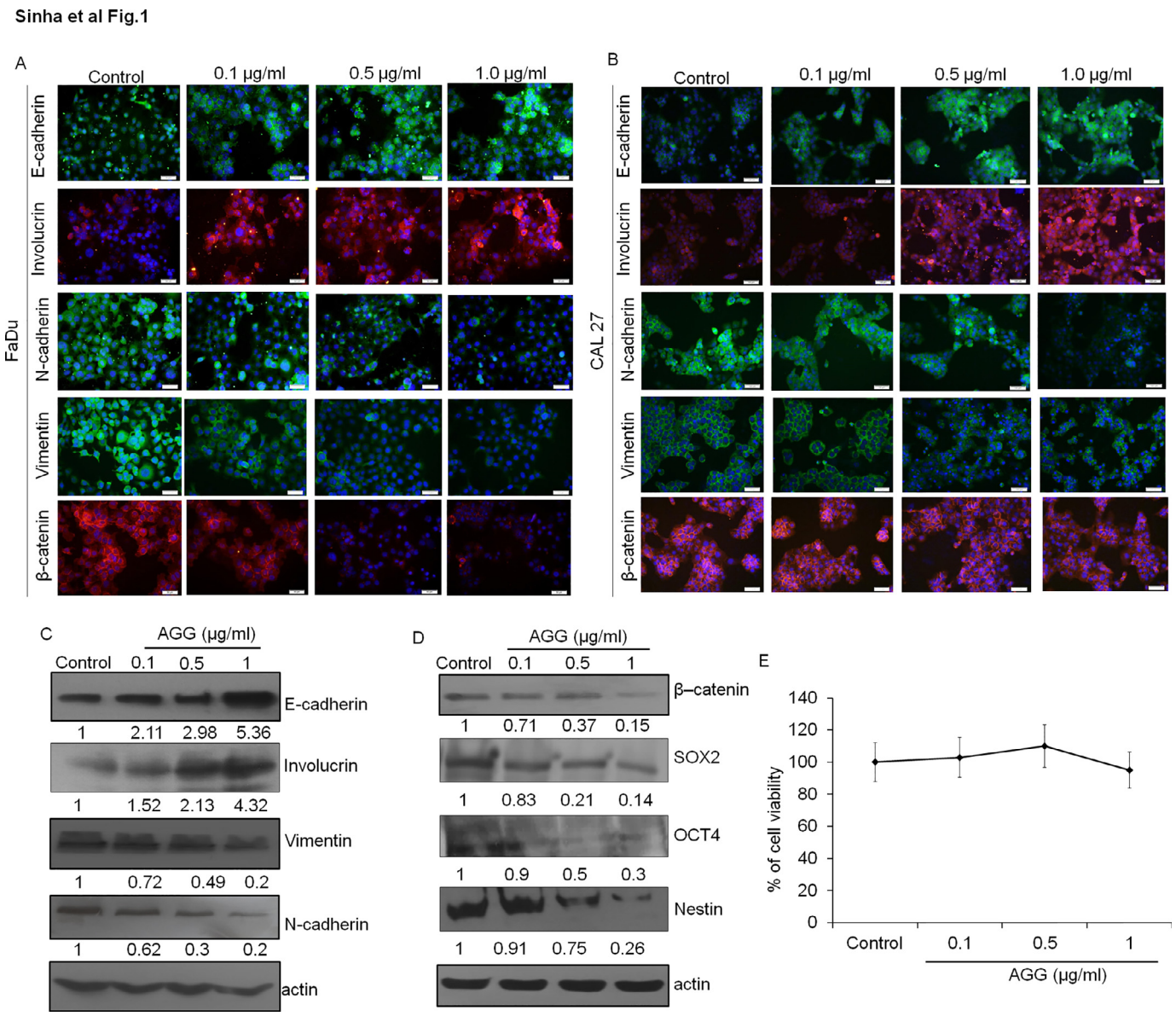

Fig. 1. AGG inhibits epithelial to mesenchymal transition and stemness in oral cancer cells. FaDu and CAL 27 cells were treated with different concentration (0.1, 0.5 and 1 μg/ml) of AGG for 24 h and analyzed for expression of E-cadherin, N-cadherin, Involucrin, Vimentin and β-catenin by fluorescence microscopy (Olympus IX71; 20×) (A and B). After 24 h of the treatment with AGG, the expression of Involucrin, E-cadherin, N-cadherin, β-catenin, Vimentin, SOX2, OCT4, Nestin and actin by was analyzed by Western Blot (C, D). IM-PHFA cells were treated with different concentration of AGG for 24 h and cell viability was performed by MTT assay (E). Data are reported as the mean ± S.D. of three independent experiments and compared against PBS control. Densitometry was performed on the original blots, considering that the ratio of protein to actin in control cells was 1.

on IM-PHFA (Fig. 1E), confirming AGG has no neurotoxic effect for possible anticancer applications.

Growth factors including EGF play an intricate role in EMT, as well as in modulating ECM degradation and facilitating the progression of oral SCC (Baulida et al., 2015). In this study, the effect of AGG on EMT, stemness, and invasive potential in EGF-stimulated FaDu cells was studied. In addition, we stimulated FaDu cells with 20 ng/ml EGF for 1 h, followed by AGG treatment and observed that the E-cadherin expression increased in a dose-dependent manner in FaDu cells (Fig. 2A). The inhibition of EMT was further shown as loss of mesenchymal markers including N-cadherin, β-catenin, and vimentin in EGF-induced FaDu cells (Fig. 2A). Interestingly, AGG considerably downregulated the expression of SOX2, OCT4, and nestin in EGF-induced FaDu cells, thereby inhibiting the pluripotency of CSCs (Fig. 2A). Furthermore, AGG prevented the tumor cell invasive property of EGF-stimulated FaDu cells by downregulating adisintegrin and metalloprotease (ADAM17), which plays an implicative role in cancer cell invasion (Fig. 2A). To emphasize our hypothesis, the invasive potential of cells was quantified by analyzing the number of HE-stained cells that enter into the lower chamber of Boyden chamber, which was decreased from 180 ± 6.5 (control) to 160 ± 6.8, 120 ± 7.6, and 80 ± 9 in instances of 0.1, 0.5, and 1 μg/ml, of AGG, respectively (Fig. 2B and C), confirming AGG as a potent EMT inhibitor in oral cancer.

Snail inhibition by AGG leads to p73-dependent E-cadherin-mediated EMT regulation

Snail promotes cell migration and invasion through the suppression of E-cadherin tumor suppressor by binding to E-boxes located in the promoter region (Baulida et al., 2015). As Snail has a short half-life period and gets degraded quickly (Zhou et al., 2004), we studied the effect of AGG on Snail expression in the presence of MG132 and data

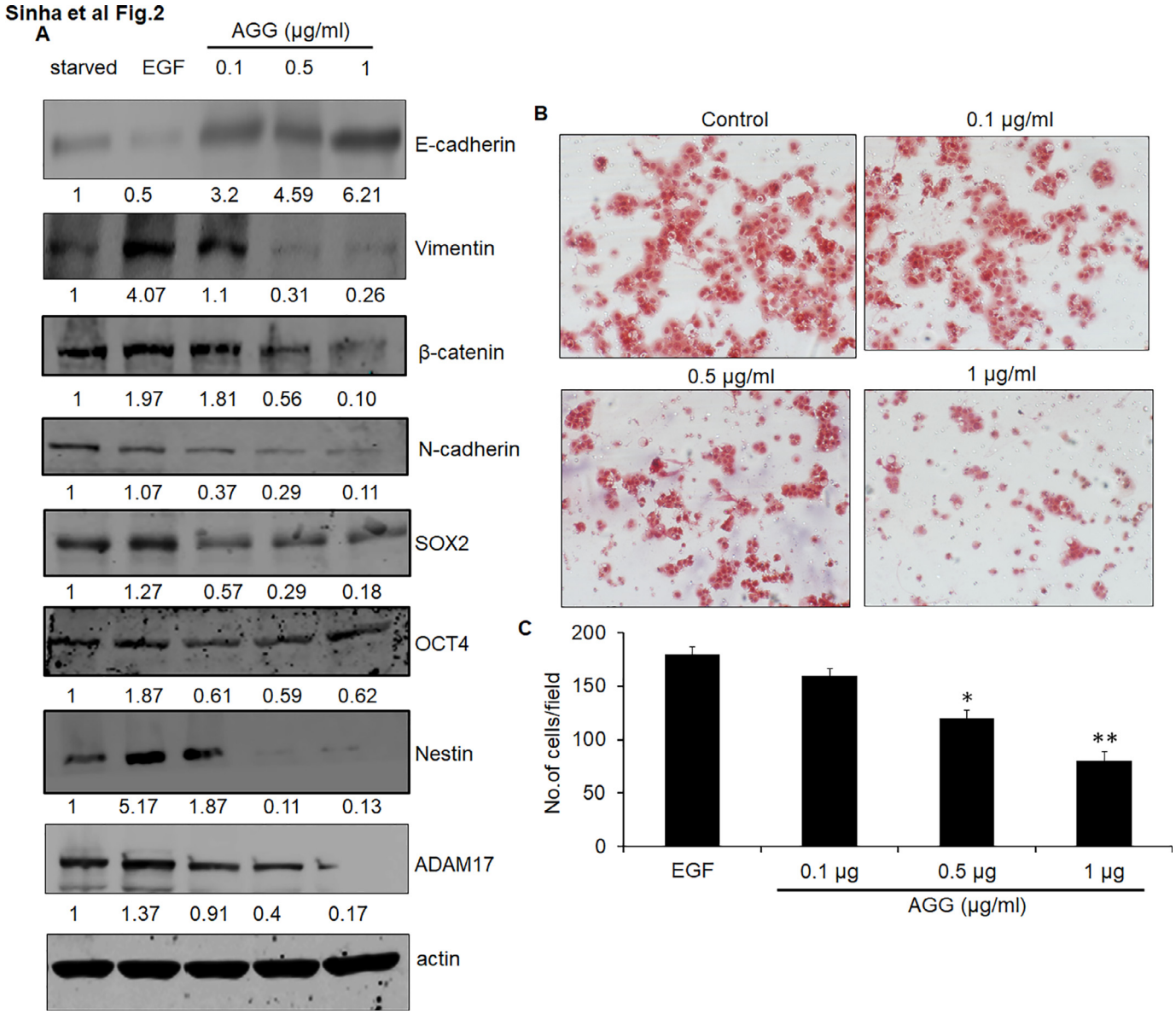

Fig. 2. AGG inhibits EGF-stimulated epithelial to mesenchymal transition and stemness in FaDu cells. After EGF (20 ng/ml) stimulation for 1 h, FaDu cells were treated with AGG (0.1, 0.5 and 1 μg/ml) for 24 h, and of the expression of E-cadherin, Vimentin, β-catenin, N-cadherin, SOX2, OCT4, Nestin and ADAM17 was followed by Western Blot (A). After 24 h of the treatment with AGG, FaDu cells were examined by invasion assay; the cells were fixed and quantified (B, C). Data are reported as the mean ± S.D. of three independent experiments and compared against PBS control. *p-value < 0.05; **p-value < 0.01 were considered significant as compared to control. Densitometry was performed on the original blots, considering that the ratio of protein to actin in control cells was 1.

showed that EGF-stimulated FaDu cells exhibiting a decreased expression of Snail upon AGG treatment (Fig. 3A). Furthermore, the down-regulation of Snail was inversely correlated with p73 expression in the presence of AGG (Fig. 3B). Our previous findings supported that AGG effectively upregulated p73 expression in FaDu cells (Sinha et al., 2017a). In this study, the altered p73 expression in Snail overexpressed EGF-stimulated FaDu cells upon AGG treatment at an effective dose (1 μg/ml; Fig. 3C and D). The overexpression of Snail inhibited cell-cell interactions and decreased E-cadherin expression (Fig. 3D). The invasive capacity of Snail overexpressed the FaDu cells, which increased with the upregulated expression of ADAM17, compared with control cells upon EGF stimulation. This indicates that Snail can be considered a master gene in the EMT because of its invasive properties conferred by the decreased cell polarity, cell dedifferentiation, changes in connections between cells, and strengthened invasive ability (Fig. 3D). Moreover, the overexpression of Snail was associated with the stemness of FaDu cells, manifested by the upregulated expression of transcription factors SOX2 responsible for maintaining the CSC-like phenotype (Fig. 3D).

The cancer cells undergoing an EMT show increased resistance to apoptosis with the potential to attain the traits of CSCs. Furthermore, the p53 family proteins have been shown to regulate EMT (Lee et al., 2009; Lim et al., 2010), and in this study, we investigated the role of p73 in AGG-inhibited EMT in FaDu cells. In addition, we transiently transfected FaDu cells with p73DD, and the p73DD-transfected FaDu cells were stimulated by EGF, followed by a treatment with an effective dose (1 μg/ml) of AGG. The data showed that the p73DD restored the Snail expression compared with that in the mock cells with a decrease in E-cadherin expression (Fig. 3E). Compared with the wild-type, the blocked expression of p73 contributed to the invasiveness, evident from ADAM17 expression in AGG-treated p73DD cells (Fig. 3E). The increased Snail expression upon AGG treatment (1 μg/ml) in p73DD cells corroborated with the upregulated transcription factors; SOX2 is responsible for the plasticity of CSCs (Fig. 3E). Henceforth, the disruption

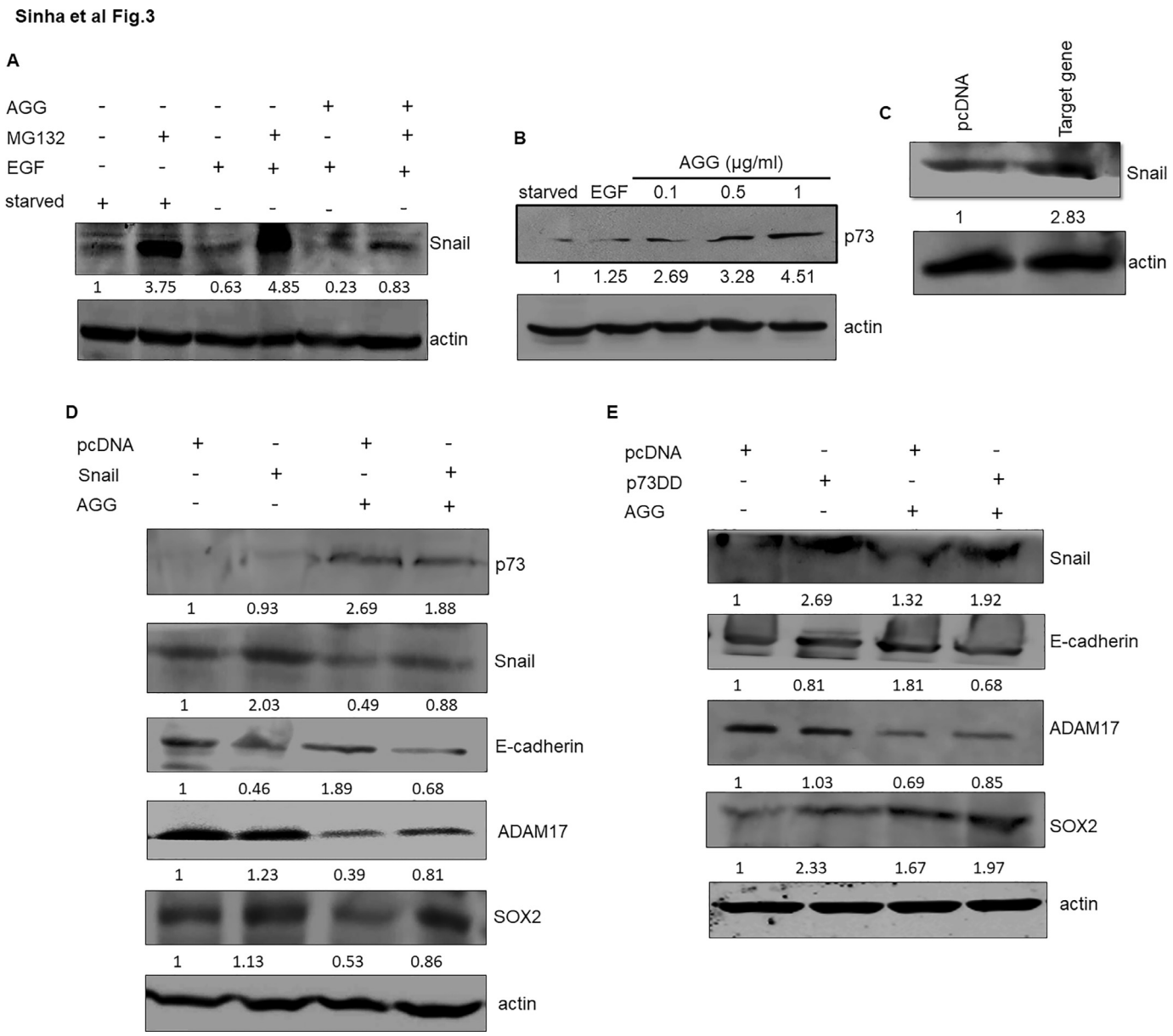

Fig. 3. Snail inhibition by AGG leads to a p73-dependent E-cadherin mediated EMT regulation in FaDu cells. FaDu cells were pre-treated with MG132 for 2 h followed by EGF stimulation and treatment with the effective dose of AGG (1 μg/ml) to monitor the Snail expression by Western Blot (A). p73 expression was monitored in AGG (0.1, 0.5, and 1 μg/ml) treated FaDu cells by Western Blot (B). FaDu cells were transfected with Snail and p73DD with empty backbone pcDNA3 and the expression of the target proteins was analyzed by Western blot (C). After 48 h of transfection, the cells were stimulated with EGF (20 ng/ml) for 1 h, and treated with an effective dose of AGG (1 μg/ml) for 24 h to study the target protein expression by Western Blot (C, D, E). Densitometry was performed on the original blots, considering that the ratio of protein to actin in control cells was 1.

of E-cadherin and p73 expression with enhanced Snail expression plays a crucial role in tumor progression, and the inhibition of Snail by AGG may have therapeutic benefits.

p73 induction leads to Snail degradation-mediated epithelial-to-mesenchymal transition inhibition

Snail has been shown to interact with tumor-associated proteins including HDAC1, DNMT1, and p53 to regulate EMT, invasion, and metastasis (Lim et al., 2010). To establish a relation between Snail and p73, we studied their direct interaction through co-immunoprecipitation. Co-immunoprecipitation studies were conducted to extract Snail and p73 from the cell lysates using anti-Snail or anti-p73 for immunoprecipitation, followed by immunoblotting with anti-p73 or anti-Snail antibody after AGG treatment in FaDu cells. The results showed that Snail interacted with p73 in EGF-induced FaDu cells, whereas AGG hindered this interactome, leading to the release of p73 from Snail sequestration to modulate EMT inhibition (Fig. 4A).

To understand the molecular interaction between the p73 domain and Snail, we performed a 10-ns-long MD simulation of the docked p73-Snail complex (Fig. 4B and C). At the end of the simulation, the complex was quite stable with a root mean square deviation value of 3 to 4.5 Å for the Cα backbone atoms (Supplementary Section Fig. S1). MM-GBSA method was used to calculate the binding free energy of p73 domain with Snail protein. The binding free energy calculated using the MM-GBSA method was − 50.561 kcal mol^{-1} for the complex (Supplementary Table 1). The favorable contribution from the direct electrostatic interactions between p73 domain and Snail was recompensed by the electrostatic desolvation free energy upon binding, which progressed to an unfavorable contribution as a whole, consistent with other MM-

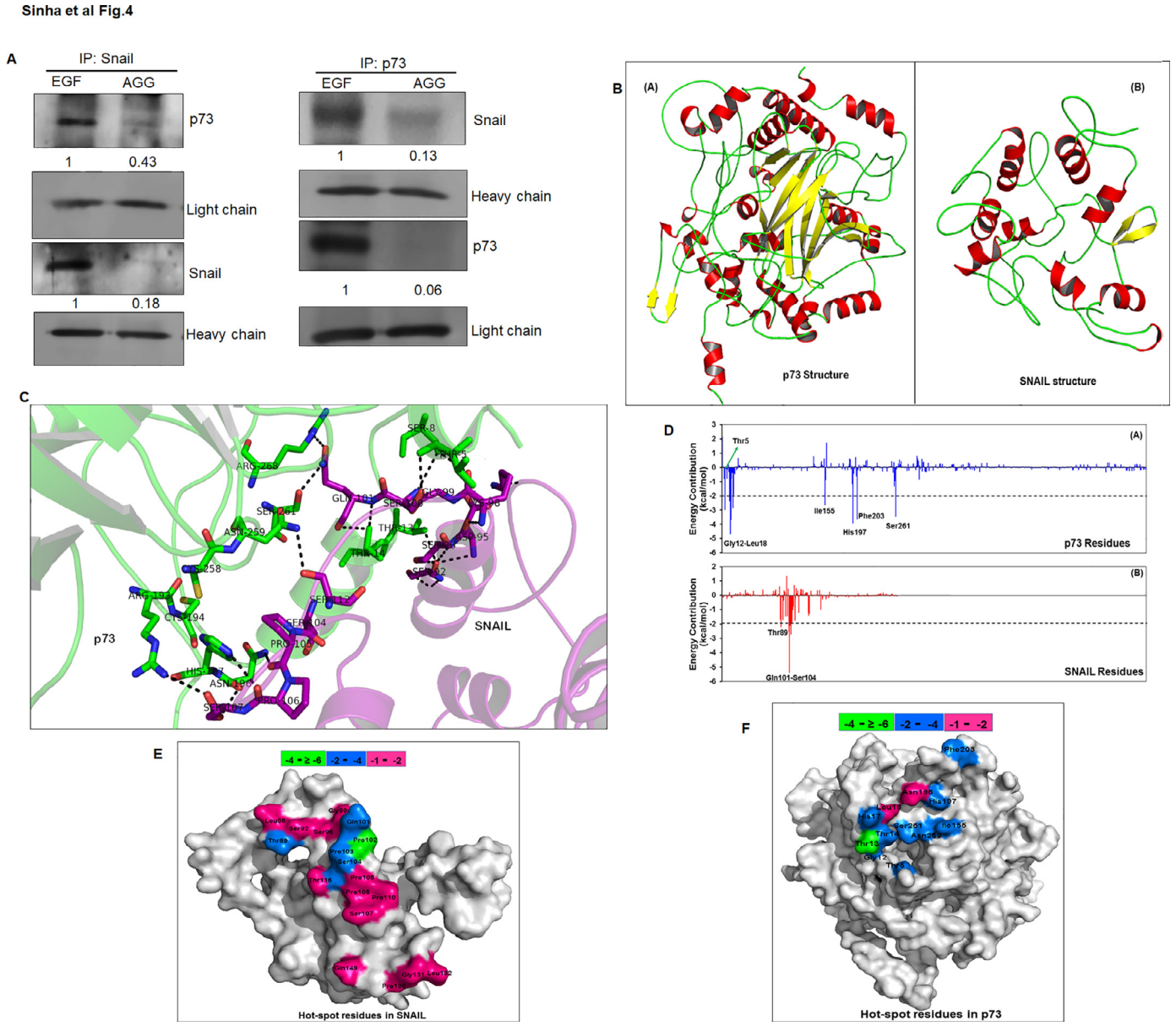

Fig. 4. Snail translocation to cytosol followed by its ubiquitination in FaDu cells. EGF (20 ng/ml) induced FaDu cells were treated with AGG for 24 h and expression of Snail was examined by confocal microscopy (Leica TCS SP8; 630×) (A). After treatment with AGG, Snail/Ub interaction in FaDu cells was studied by immunoprecipitation analysis. Data are reported as of three independent experiments and compared against PBS control. Densitometry was performed on the original blots, considering that the ratio of protein to actin in control cells was 1.

GBSA and MM-PBSA studies. In contrast, nonpolar interactions, $\Delta G_{nonpolar}$ (including van der Waals interactions and nonpolar solvation), contribute − 154.291 kcal mol^{-1}, which is highly favorable for the binding process and consistent with the large hydrophobic binding surface between p73 domain and Snail. Through the decomposition of the binding free energy into the individual contribution from each residue, it was possible to recognize the binding hotspots for p73 domain and Snail (Fig. 4D). In addition, this showed that the several residues of p73 domain favorably contribute more than − 2.0 kcal mol^{-1}: Thr5, Gly12, Thr13, Thr14, His17, Ile155, His197, Phe203, and Ser261. Moreover, some other residues (including Asn196, Asn259, and Ser260) contribute more than − 1 kcal mol^{-1} (Fig. 4E). These key residues of p73 domain that interact with Snail are mainly from the very first α-helix from the N-terminus and the connecting loops between the first and second antiparallel beta-sheets pair. Furthermore, in Snail, Thr89, Gln101, Pro102, Pro103, and Ser103 each contribute more than − 2.0 kcal mol^{-1} of the free energy, whereas Leu88, Ser92, Ser96, Gly99, Pro105, Pro106, Ser107, Pro110, Thr116, Pro130, Gly131, Leu132, Gly133, and Gln149 contribute more than − 1 kcal mol^{-1} of the free energy (Fig. 4F). In addition, it was found that these crucial residues on the Snail surface are mainly from the second α-helix and the connecting loop between the second and third α-helix in the core region.

We further determined the mechanism of decreased expression of Snail in AGG-treated FaDu cells. The confocal microscopy data showed that the Snail protein was mainly localized in the nucleus of EGF-induced FaDu cells, whereas it was mostly found in the cytoplasm of AGG-treated cells, indicating that AGG resulted in the translocation of Snail from the nucleus to the cytoplasm in FaDu cells (Fig. 5A). Furthermore, we observed that Snail was considerably ubiquitinated in FaDu cells in the AGG-treated group compared with that in control group (Fig. 5B), concluding the disruption of Snail-p73 interaction by AGG leading to the cytoplasmic translocation of Snail and degradation through ubiquitination to cause EMT inhibition.

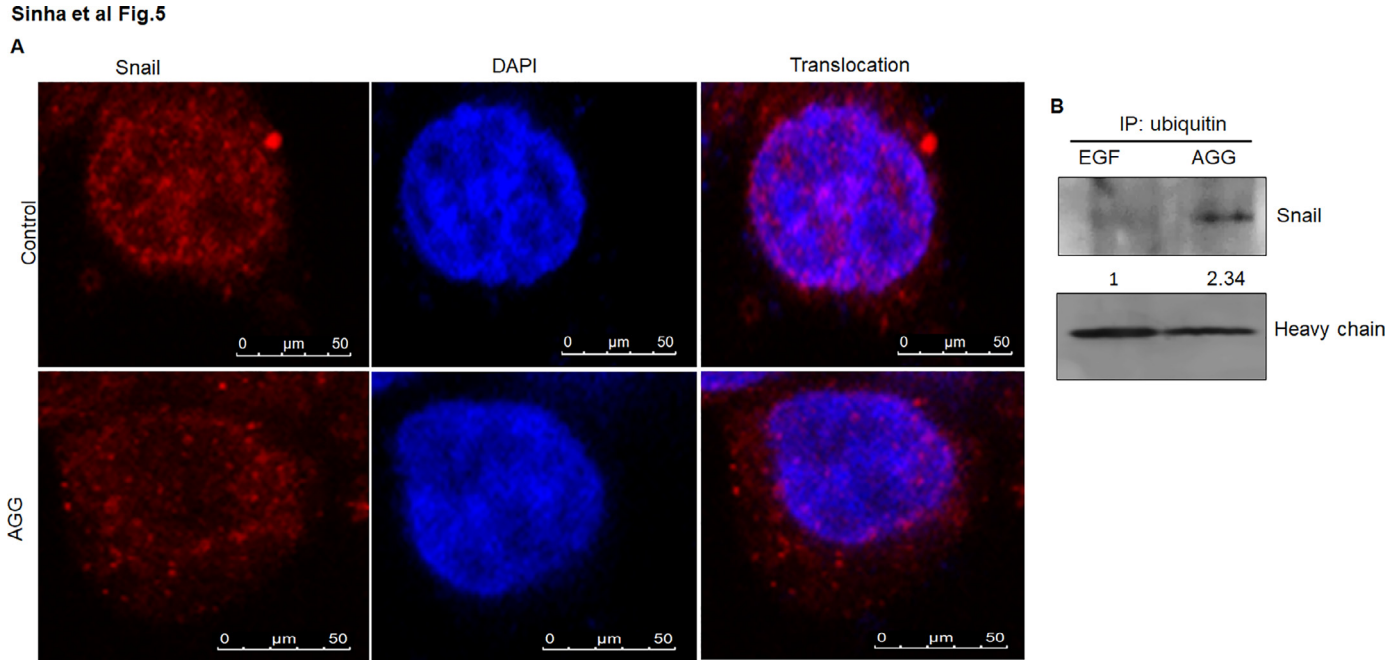

Fig. 5. Snail interacts with p73. FaDu cells were treated with AGG for 24 h and immunoprecipitated with anti–p73or anti–Snail followed by immunoblotting with anti–Snail or anti–p73 antibodies (A). Data are reported of three independent experiments and compared against PBS control. Densitometry was performed on the original blots, considering that the ratio of protein to actin in control cells was 1. A schematic ribbon representation of the predicted structures of (A) p73 and (B) Snail from *ab initio* modeling by I-TASSER protein structure prediction software is given. A schematic ribbon representation of the p73-Snail complex structure is shown in different colors. P73 domain is shown in green color while the Snail structure is shown in purple color. Residues showing the interactions are shown as sticks along domain interface for both p73 and Snail. Black dashed lines show the polar contacts between the residues. The decomposition of ΔG on a per-residue basis or the pair interaction energy between p73 domain and Snail: (a) the contribution of each residue in p73 to Snail domain binding; (b) the contribution of each residue in Snail to p73 domain binding. The distributions of the identified hotspot residues on the p73 domain in surface representation. Colored bars show the range of contributions by residues in the unit kcal/mol. The distributions of the identified hotspot residues on the Snail in surface representation. Colored bars show the range of contributions by residues in the unit kcal/mol.

AGG regulates EMT, stemness, and invasion through ERK inhibition

Cytoplasmic/nuclear β-catenin expression has been found to considerably associate with EGFR expression in OSCC (Zhang et al., 2014). The EGFR overexpression has been demonstrated in approximately 90% of head and neck cancers (Mishima et al., 1998; Gkouveris et al., 2014), and our data showed the downregulation of EGFR in AGG-treated EGF-induced FaDu cells in a dose-dependent manner (Fig. 6A). Furthermore, the oral SCC has been reported to use alternative signaling pathways including PI3K/Akt, MEK/ERK, or Wnt/β-catenin pathway for tumor progression. In the presence of different growth signals including EGF, Snail expression is modulated through ERK and serine/threonine kinases, resulting in increased cell spreading and greatly enhanced cell survival. This study showed that AGG downregulated the activated ERK1/2 in response to EGF stimulation in FaDu cells (Fig. 6B). On introduction of PD98059, a highly selective flavonoid that specifically binds to the inactive forms of MEK1 and inhibits both MEK 1 and MEK2 activation *in vitro* with varying IC_{50} values ameliorated ERK inhibition in the presence of AGG (Fig. 6C). In addition, the downstream molecule of ERK and Snail expression decreased in FaDu cells. Following the downregulation of Snail, E-cadherin, one of the structural proteins regarded as caretakers of the epithelial phenotype, was upregulated shunting the expression of SOX2, OCT4, and nestin transcriptional factors responsible for the stemness and invasive marker ADAM17 in EGF-stimulated FaDu cells (Fig. 6D). The molecular mechanisms involved in ERK1/2-mediated EMT inhibition and cell death in oral cancer are largely unknown. In this study, data showed that AGG deactivated ERK1/2 and prompted an increased p73 expression in EGF-induced FaDu cells, concluding that p73 acts downstream of MEK activation and plays a crucial role in Snail inhibition.

Effect of AGG on the expression of EMT modulators in FaDu xenograft tissue

To further uphold our *in vitro* finding under *in vivo* conditions, we then examined the effect of AGG on the expression of E-cadherin, Snail, p73, vimentin, and SOX2 in FaDu xenograft tissues. In a previous study, we investigated that AGG strongly (50 µg/kg body weight) inhibited the xenograft tumors of FaDu cells in athymic nude mice. The tumor tissues were subjected to immunohistochemistry analysis to examine the status of molecules involved in the EMT and stemness. In addition, the analysis of FaDu xenograft tissue sections revealed that there was a remarkable increase in the expression of E-cadherin and p73 with a decrease in the expression of Snail, vimentin, and SOX2 in the AGG-treated group compared with that in the control group (Fig. 7A). The immunoreactivity score clearly distinguished the expression of E-cadherin as low and moderate, p73 as low and high in control and treated groups, and Snail as moderate and low in control and treated groups, followed by vimentin and SOX2 with high and low immunoreactivity score in the control and treated groups (Fig. 7B). Overall, these findings suggest that AGG suppressed the expression of the mesenchymal phenotypes and stemness *in vivo* along with the upregulation of E-cadherin and p73 as a part of its anticancer efficacy against HNSCC (Fig. 7C).

Discussion

Despite progress in the available successive treatments, oral cancer is associated with high morbidity and poor prognosis because of local invasiveness and distant metastasis (Sinha et al., 2013; Naik et al., 2016). The metastasis progression is due to the aggressive phenotypical change through the induction of EMT, and the inhibition of EMT can be a critical strategy for preventing or delaying cancer progression (Li et al., 2013; Lee et al., 2015; Pan et al., 2015; Su et al., 2015; Jiao et al.,

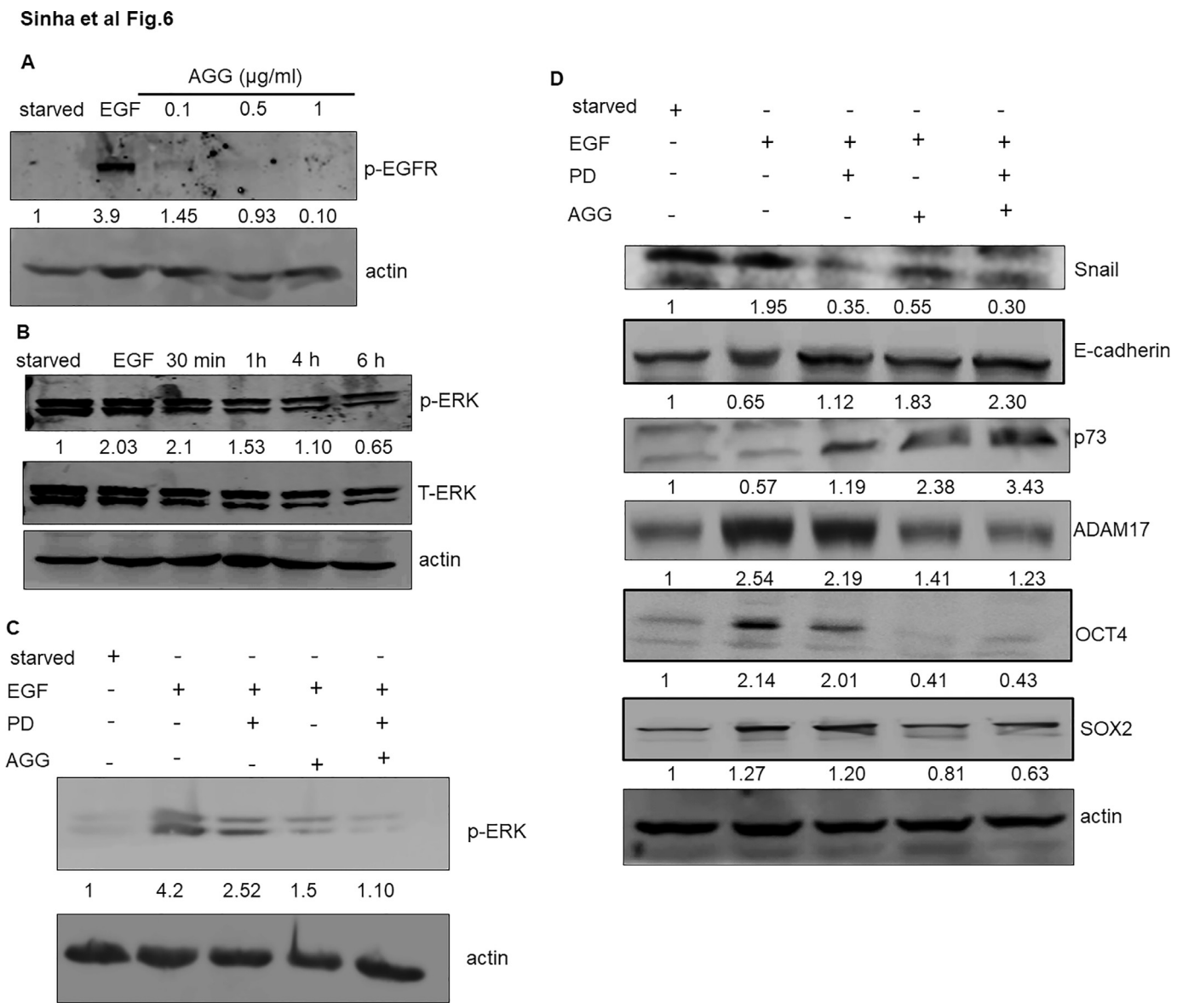

Fig. 6. AGG regulates EMT, stemness, invasiveness through ERK inhibition. FaDu cells were stimulated with EGF (20 ng/ml) for 1 h and were treated with AGG for 24 h and the expression of EGFR was examined by Western blot (A). After treatment with AGG (1 μg/ml), FaDu cells were analyzed for ERK expression by Western blot (B). On introduction of PD98059, a highly selective flavonoid that specifically binds to inactive forms of MEK1, the expression of ERK in presence of effective dose of AGG (1 μg/ml) was monitored (C), followed by evaluation of Snail, E-cadherin, p73, ADAM17, OCT4, and SOX2 by Western Blot (D). Data reported as three independent experiments and compared against PBS control. Densitometry was performed on the original blots, considering that the ratio of protein to actin in control cells was 1.

2016). Phytotherapeutic agents with multiple molecular targets can be a novel effective drug for metastatic oral cancer. Natural molecules including curcumin (Lee et al., 2015; Jiao et al., 2016), plumbagin (Pan et al., 2015), pterostilbene (Su et al., 2015), and resveratrol (Li et al., 2013) have been successfully established as anti-invasive and anti-metastatic compounds. AGG displays potent anticancer activities through its inhibitory effects on multiple signaling pathways, including angiogenesis, autophagy, and apoptosis. In this study, AGG treatment can reduce EMT progression with the re-establishment of E-cadherin expression, followed by Snail inhibition, and rescued apoptotic potential of inactivated p73 in oral cancer (Fig. 8).

EMT is a key step toward cancer progression through the loss of E-cadherin expression in different types of cancer including oral cancer (Smith et al., 2013). Interestingly, the overexpression of E-cadherin in the invasive carcinoma of colorectal cancer can inhibit metastatic abilities (Lee et al., 2012). Furthermore, CSCs can display EMT phenotypes with the loss of E-cadherin expression, and these stem cells may migrate to a distant site and be responsible for metastatic relapse, particularly after cancer surgery (Zhu et al., 2012; Zhang et al., 2014). Our data revealed that AGG inhibited the cells undergoing EMT, characterized by the upregulation of E-cadherin and involucrin and downregulation of N-cadherin and vimentin in different types of oral cancer cells. Subsequently, CSC markers were quantified in oral cancer cells, and data showed that the expression of OCT4, SOX2, and β-catenin decreased upon AGG treatment. Notably, we demonstrated the ability of AGG to inhibit the acquisition of mesenchymal phenotype and stemness *in vivo*, indicating AGG targets both EMT and stemness as part of its anticancer efficiency in oral cancer.

Several transcription factors have been implicated in the suppression of E-cadherin expression including Snail, ZEB–1, Slug, and Twist. The loss of E-cadherin expression is influential because of the overexpression of Snail or Twist that plays a distinct role in tumor

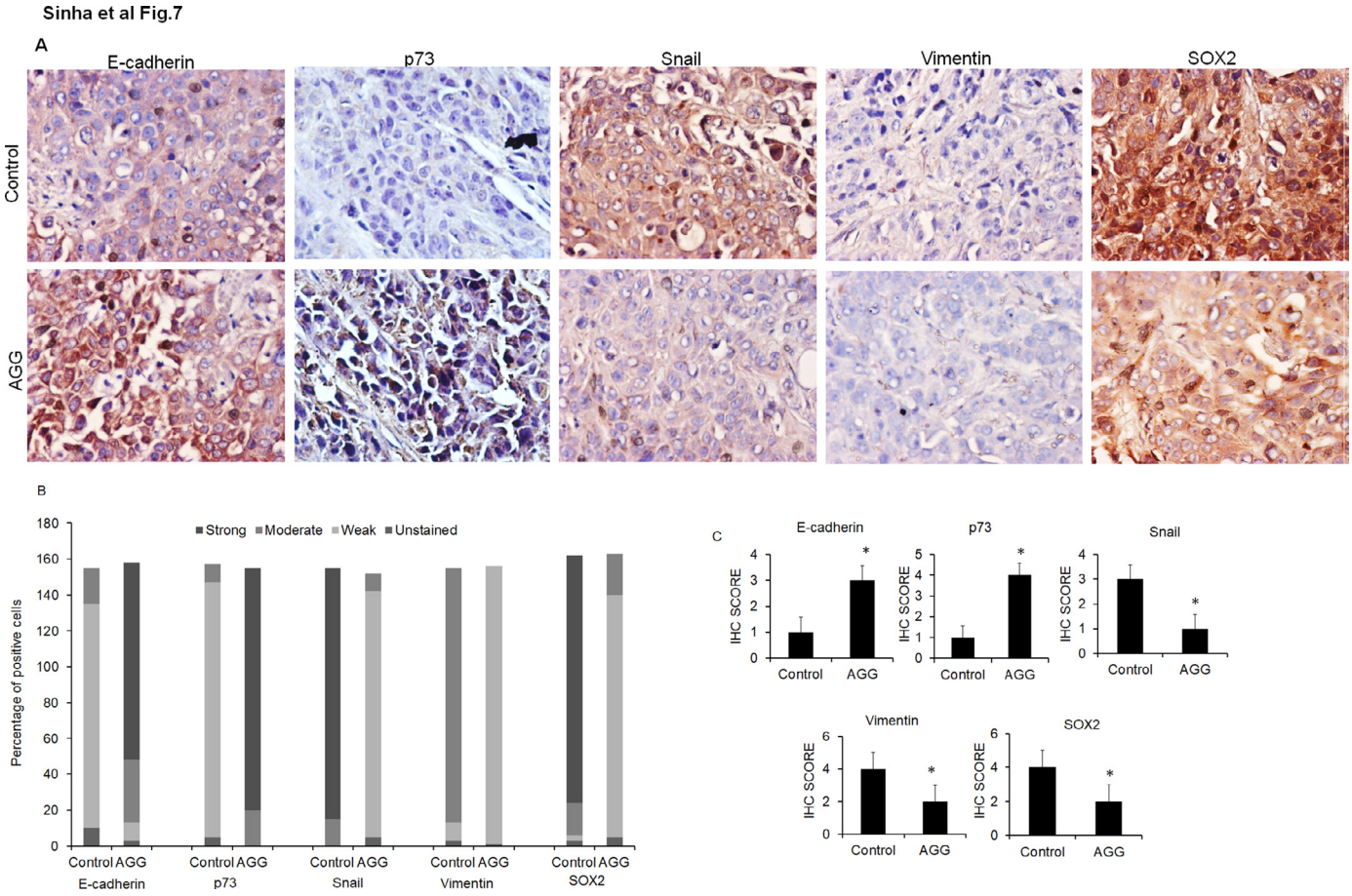

Fig. 7. AGG inhibits the expression of EMT regulators and stemness in FaDu xenograft tissue. FaDu xenograft tissues were harvested followed by fixation with formalin and paraffin-embedded sections were immunostained for E-cadherin, p73, Snail, Vimentin, and SOX2 in control and treated groups (A). The semi-quantitative immunoreactive analysis of PCNA and active caspase–3 was carried out by histoscore method (C). Data are reported as the mean ± S.D. of three independent experiments and compared against PBS control. *p value < 0.05 was considered significant as compared to control.

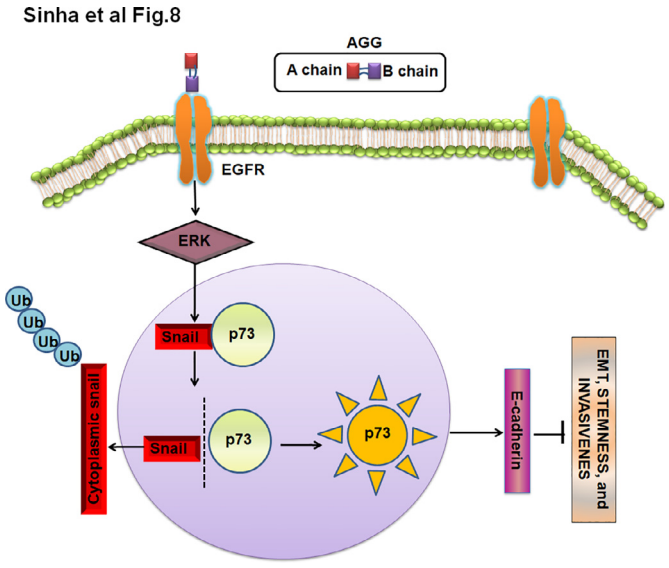

Fig. 8. A flowchart depicting the mechanism of snail degradation by AGG is given. AGG treatment in EGF-induced FaDu cells induces p73 activation and inhibits Snail-p73 interaction for Snail degradation resulting in the upregulation of epithelial marker and downregulation of mesenchymal markers and stemness.

progression identified in various types of epithelial tumors, including gastric, prostate, breast, and head and neck cancers (Baritaki et al., 2009; Lim et al., 2010; Smith et al., 2013 Zander et al., 2014; Smith et al., 2014). In addition, the overexpression of Snail in the nonmetastatic LNCaP cells resulted in EMT induction and acquisition of more mesenchymal phenotype than the wild-type cells (Baritaki et al., 2009). AGG controlled the Snail-mediated EMT and thus restricted the ability of tumor cells to invade and metastasize, with a decrease in the expression of ADAM17 in EGF-induced FaDu cells. Interestingly, the overexpression of Snail in FaDu cells modulated EMT and E-cadherin expression in the presence of AGG. The tumor suppressor p53 family proteins play crucial roles in controlling cancer invasion and metastasis (Powell et al., 2014). For example, p53 knockdown in hepatocellular carcinoma cells played a pivotal role in EMT and metastasis through its regulation *in vitro* and *in vivo* by modifying β-catenin signaling (Lim et al., 2010). Another member p73 acts as a negative regulator of EMT for maintaining the normal cell polarity in mammary epithelial cells (Zhang et al., 2012). In association with this, this study showed that AGG-induced p73 inhibited EMT and invasion in FaDu cells, which was reversed in p73-deficient FaDu cells. A previous study showed that curcumin treatment stimulated p53 expression to inhibit EMT and metastasis in oral SCC (Lee et al., 2015). The activation of EMT through Snail has been observed to be associated with ERK signaling in cancer and the inhibition of p-ERK with UO126 that resulted in a decrease in Snail expression and reverted EMT in breast cancer (Smith et al., 2014). Notably, a natural compound Oroxylin A inhibited EMT by suppressing ERK/GSK–3β/Snail signaling in nonsmall-cell lung cancer cells

(Wei et al., 2016). Accordingly, this study showed that AGG attenuated the activation of ERK1/2 to reduce the Snail level in EGF-stimulated FaDu cells for regulating EMT as a promising process for targeting tumor metastasis.

The degradation of Snail to regulate the protein level plays a crucial role in inhibiting Snail-induced tumor malignancy. For instance, FBXO11 promoted the ubiquitination and degradation of Snail through protein kinase D1 phosphorylation at Ser–11 in Snail to inhibit Snail-dependent EMT and metastasis in multiple breast cancer cells (Zheng et al., 2014). Similarly, the interaction between the Notch1 intracellular domain and Snail resulted in the MDM2-dependent degradation of Snail to block Snail-regulated invasive properties in hepatocellular carcinoma (Lim et al., 2011). Moreover, the degradation of Snail/Slug is controlled by p53 protein (Lim et al., 2010). Although p73 plays a role in EMT, its association with Snail has not been interpreted previously. This study showed that AGG-induced p73 has an essential role in Snail translocation and degradation to regulate EMT in FaDu cells. The molecular mechanism of p73-dependent Snail degradation and contribution of key molecules in this process to inhibit EMT are yet to be investigated. In conclusion, AGG inhibits invasion and stemness through Snail degradation in a p73-dependent pathway (Fig. 8), which may be a potent therapeutic agent for a metastatic tumor in oral cancer.

Conflict of interest

The authors have declared no conflict of interest.

Acknowledgments

Research support was partly provided by Council of Scientific and Industrial Research (CSIR) [Number: 37(1608)/13/EMR-II], Human Resource Development Group and Science and Technology Department, Government of Odisha. Research infrastructure was partly provided by Fund for Improvement of S&T infrastructure in universities & higher educational institutions (FIST) [Number: SR/FST/LSI-025/2014], Department of Science and Technology, Government of India. BRM is thankful to Supercomputer Education and Research Centre (SERC) at Indian Institute of Science (IISc) Bangalore for high performance computing facilities and BUILDER project (BT/PR-9028/INF/22/193/2013) by Department Biotechnology (DBT) for financial assistance.

Supplementary materials

Supplementary material associated with this article can be found, in the online version, at doi:10.1016/j.phymed.2018.08.003.

References

Baritaki, S., Chapman, A., Yeung, K., Spandidos, D.A., Palladino, M., Bonavida, B., 2009. Inhibition of epithelial to mesenchymal transition in metastatic prostate cancer cells by the novel proteasome inhibitor, NPI-0052: pivotal roles of Snail repression and RKIP induction. Oncogene 28, 3573–3585.

Baulida, J., García de. Herreros, A., 2015. Snail1-driven plasticity of epithelial and mesenchymal cells sustains cancer malignancy. Biochim. Biophys. Acta 1856, 55–61.

Behera, B., Devi, K.S., Mishra, D., Maiti, S., Maiti, T.K., 2014a. Biochemical analysis and antitumour effect of Abrus precatorius agglutinin derived peptides in Ehrlich's ascites and B16 melanoma mice tumour model. Environ. Toxicol. Pharmacol. 38, 288–296.

Behera, B., Mishra, D., Roy, B., Devi, K.S., Narayan, R., Das, J., Ghosh, S.K., Maiti, T.K., 2014b. *Abrus precatorius* agglutinin-derived peptides induce ROS-dependent mitochondrial apoptosis through JNK and Akt/P38/P53 pathways in HeLa cells. Chem. Biol. Interact. 222, 97–105.

Bhutia, S.K., Behera, B., Das, D.N., Mukhopadhyay, S., Sinha, N., Panda, P.K., Naik, P.P., Patra, S.K., Mandal, M., Sarkar, S., Menezes, M.E., Talukdar, S., Maiti, T.K., Das, S.K., Sarkar, D., Fisher, P.B., 2016. Abrus agglutinin is a potent anti-proliferative and anti-angiogenic agent in human breast cancer. Int. J. Cancer 139, 457–466.

Bhutia, S.K., Mallick, S.K., Maiti, S., Maiti, T.K., 2008a. Antitumor and proapoptotic effect of Abrus agglutinin derived peptide in Dalton's lymphoma tumor model. Chem. Biol. Interact. 174, 11–18.

Bhutia, S.K., Mallick, S.K., Stevens, S.M., Prokai, L., Vishwanatha, J.K., Maiti, T.K., 2008b. Induction of mitochondria-dependent apoptosis by Abrus agglutinin derived peptides in human cervical cancer cell. Toxicol. In Vitro 22, 344–351.

Cao, M.X., Jiang, Y.P., Tang, Y.L., Liang, X.H., 2016. The crosstalk between lncRNA and microRNA in cancer metastasis: orchestrating the epithelial-mesenchymal plasticity. Oncotarget 8, 12472–12483.

Chang, C.J., Chao, C.H., Xia, W., Yang, J.Y., Xiong, Y., Li, C.W., Yu, W.H., Rehman, S.K., Hsu, J.L., Lee, H.H., Liu, M., Chen, C.T., Yu, D., Hung, M.C., 2011. p53 regulates epithelial-mesenchymal transition and stem cell properties through modulating miRNAs. Nat. Cell Biol. 13, 317–323.

Comeau, S.R., Gatchell, D.W., Vajda, S., Camacho, C.J., 2004. ClusPro: a fully automated algorithm for protein-protein docking. Nucleic Acids Res 32, W96–W99.

Fernandez-Alonso, R., Martin-Lopez, M., Gonzalez-Cano, L., Garcia, S., Castrillo, F., Diez-Prieto, I., Fernandez-Corona, A., Lorenzo-Marcos, M.E., Li, X., Claesson-Welsh, L., Marques, M.M., Marin, M.C., 2015. p73 is required for endothelial cell differentiation, migration and the formation of vascular networks regulating VEGF and TGFβ signaling. Cell Death Differ. 22, 1287–1299.

Fernandez-Garcia, B., Vaqué, J.P., Herreros-Villanueva, M., Marques-Garcia, F., Castrillo, F., Fernandez-Medarde, A., León, J., Marín, M.C., 2007. p73 cooperates with Ras in the activation of MAP kinase signaling cascade. Cell Death Differ. 14, 254–265.

Ghosh, D., Maiti, T.K., 2007. Immunomodulatory and anti-tumor activities of native and heat denatured Abrus agglutinin. Immunobiology 212, 589–599.

Gkouveris, I., Nikitakis, N., Karanikou, M., Rassidakis, G., Sklavounou, A., 2014. Erk1/2 activation and modulation of STAT3 signaling in oral cancer. Oncol. Rep. 32, 2175–2182.

Hegde, R., Maiti, T.K., Podder, S.K., 1991. Purification and characterization of three toxins and two agglutinins from Abrus precatorius seed by using lactamyl-Sepharose affinity chromatography. Anal. Biochem. 194, 101–109.

Jiao, D., Wang, J., Lu, W., Tang, X., Chen, J., Mou, H., Chen, Q.Y., 2016. Curcumin inhibited HGF-induced EMT and angiogenesis through regulating c-Met dependent PI3K/Akt/mTOR signaling pathways in lung cancer. Mol. Ther. Oncolytics 3, 16018.

Lee, A.Y., Fan, C.C., Chen, Y.A., Cheng, C.W., Sung, Y.J., Hsu, C.P., Kao, T.Y., 2015. Curcumin inhibits invasiveness and epithelial-mesenchymal transition in oral squamous cell carcinoma through reducing matrix metalloproteinase 2, 9 and modulating p53-E-cadherin pathway. Integr. Cancer Ther. 14, 484–490.

Lee, C.C., Chen, W.S., Chen, C.C., Chen, L.L., Lin, Y.S., Fan, C.S., Huang, T.S., 2012. TCF12 protein functions as transcriptional repressor of E-cadherin, and its overexpression is correlated with metastasis of colorectal cancer. J. Biol. Chem. 287, 2798–2809.

Lee, S.H., Lee, S.J., Jung, Y.S., Xu, Y., Kang, H.S., Ha, N.C., Park, B.J., 2009. Blocking of p53-Snail binding, promoted by oncogenic K-Ras, recovers p53 expression and function. Neoplasia 11, 22–31.

Li, W., Ma, J., Ma, Q., Li, B., Han, L., Liu, J., Xu, Q., Duan, W., Yu, S., Wang, F., Wu, E., 2013. Resveratrol inhibits the epithelial-mesenchymal transition of pancreatic cancer cells via suppression of the PI-3K/Akt/NF-κB pathway. Curr. Med. Chem. 20, 4185–4194.

Lim, S.O., Kim, H., Jung, G., 2010. p53 inhibits tumor cell invasion via the degradation of snail protein in hepatocellular carcinoma. FEBS Lett. 584, 2231–2236.

Lim, S.O., Kim, H.S., Quan, X., Ahn, S.M., Kim, H., Hsieh, D., Seong, J.K., Jung, G., 2011. Notch1 binds and induces degradation of Snail in hepatocellular carcinoma. BMC Biol. 9, 83.

Mishima, K., Yamada, E., Masui, K., Shimokawara, T., Takayama, K., Sugimura, M., Ichijima, K., 1998. Overexpression of the ERK/MAP kinases in oral squamous cell carcinoma. Mod. Pathol. 11, 886–891.

Mukhopadhyay, S., Panda, P.K., Das, D.N., Sinha, N., Behera, B., Maiti, T.K., Bhutia, S.K., 2014. Abrus agglutinin suppresses human hepatocellular carcinoma *in vitro* and *in vivo* by inducing caspase-mediated cell death. Acta Pharmacol. Sin. 35, 814–824.

Naik, P.P., Das, D.N., Panda, P.K., Mukhopadhyay, S., Sinha, N., Praharaj, P.P., Agarwal, R., Bhutia, S.K., 2016. Implications of cancer stem cells in developing therapeutic resistance in oral cancer. Oral Oncol. 62, 122–135.

Ng, K.Y., Chan, L.H., Chai, S., Tong, M., Guan, X.Y., Lee, N.P., Yuan, Y., Xie, D., Lee, T.K., Dusetti, N.J., Carrier, A., Ma, S., 2017. TP53INP1 downregulation activates a p73-dependent DUSP10/ERK signaling pathway to promote metastasis of hepatocellular carcinoma. Cancer Res. 77, 4602–4612.

Pan, S.T., Qin, Y., Zhou, Z.W., He, Z.X., Zhang, X., Yang, T., Yang, Y.X., Wang, D., Zhou, S.F., Qiu, J.X., 2015. Plumbagin suppresses epithelial to mesenchymal transition and stemness via inhibiting Nrf2-mediated signaling pathway in human tongue squamous cell carcinoma cells. Drug Des. Devel. Ther. 9, 5511–5551.

Panda, P.K., Behera, B., Meher, B.R., Das, D.N., Mukhopadhyay, S., Sinha, N., Naik, P.P., Roy, B., Das, J., Paul, S., Maiti, T.K., Agarwal, R., Bhutia, S.K., 2017. Abrus Agglutinin, a type II ribosome inactivating protein inhibits Akt/PH domain to induce endoplasmic reticulum stress mediated autophagy-dependent cell death. Mol. Carcinog. 56, 389–401.

Powell, E., Piwnica-Worms, D., Piwnica-Worms, H., 2014. Contribution of p53 to metastasis. Cancer Discov. 4, 405–414.

Sinha, N., Mukhopadhyay, S., Das, D.N., Panda, P.K., Bhutia, S.K., 2013. Relevance of cancer initiating/stem cells in carcinogenesis and therapy resistance in oral cancer. Oral Oncol. 49, 854–862.

Sinha, N., Panda, P.K., Das, D.N., Mukhopadhyay, S., Naik, P.P., Maiti, T.K., Shanmugam, M.K., Chinnathambi, A., Zayed, M.E., Alharbi, S.A., Sethi, G., Bhutia, S.K., 2017a. Abrus agglutinin induces irreparable DNA damage via ROS generation followed by p73 mediated apoptosis in oral squamous cell carcinoma. Mol. Carcinog. 56, 2400–2413.

Sinha, N., Panda, P.K., Naik, P.P., Maiti, T.K., Bhutia, S.K., 2017b. Abrus agglutinin targets cancer stem-like cells by eliminating self-renewal capacity accompanied with apoptosis in oral squamous cell carcinoma. Tumour Biol. 39, 1010428317701634.

Smith, A., Teknos, T.N., Pan, Q., 2013. Epithelial to mesenchymal transition in head and neck squamous cell carcinoma. Oral Oncol. 49, 287–292.

Smith, B.N., Burton, L.J., Henderson, V., Randle, D.D., Morton, D.J., Smith, B.A.,

Taliaferro-Smith, L., Nagappan, P., Yates, C., Zayzafoon, M., Chung, L.W., Odero-Marah, V.A., 2014. Snail promotes epithelial mesenchymal transition in breast cancer cells in part via activation of nuclear ERK2. PLoS One 9, e104987.

Steder, M., Alla, V., Meier, C., Spitschak, A., Pahnke, J., Fürst, K., Kowtharapu, B.S., Engelmann, D., Petigk, J., Egberts, F., Schäd-Trcka, S.G., Gross, G., Nettelbeck, D.M., Niemetz, A., Pützer, B.M., 2013. DNp73 exerts function in metastasis initiation by disconnecting the inhibitory role of EPLIN on IGF1R-AKT/STAT3 signaling. Cancer Cell 24, 512–527.

Su, C.M., Lee, W.H., Wu, A.T., Lin, Y.K., Wang, L.S., Wu, C.H., Yeh, C.T., 2015. Pterostilbene inhibits triple-negative breast cancer metastasis via inducing microRNA-205 expression and negatively modulates epithelial-to-mesenchymal transition. J. Nutr. Biochem. 26, 675–685.

Thakur, A.K., Nigri, J., Lac, S., Leca, J., Bressy, C., Berthezene, P., Bartholin, L., Chan, P., Calvo, E., Iovanna, J.L., Vasseur, S., Guillaumond, F., Tomasini, R., 2016. TAp73 loss favors Smad-independent TGF-β signaling that drives EMT in pancreatic ductal adenocarcinoma. Cell Death Differ. 23, 1358–1370.

Wei, L., Yao, Y., Zhao, K., Huang, Y., Zhou, Y., Zhao, L., Guo, Q., Lu, N., 2016. Oroxylin A inhibits invasion and migration through suppressing ERK/GSK-3β signaling in snail-expressing non-small-cell lung cancer cells. Mol. Carcinog. 55, 2121–2134.

Zander, M.A., Burns, S.E., Yang, G., Kaplan, D.R., Miller, F.D., 2014. Snail coordinately regulates downstream pathways to control multiple aspects of mammalian neural precursor development. J. Neurosci. 34, 5164–5175.

Zhang, Y., Yan, W., Jung, Y.S., Chen, X., 2012. Mammary epithelial cell polarity is regulated differentially by p73 isoforms via epithelial-to-mesenchymal transition. J. Biol. Chem. 287, 17746–17753.

Zhang, Z., Dong, Z., Lauxen, I.S., Filho, M.S., Nör, J.E., 2014. Endothelial cell-secreted EGF induces epithelial to mesenchymal transition and endows head and neck cancer cells with stem-like phenotype. Cancer Res. 74, 2869–2881.

Zheng, H., Shen, M., Zha, Y.L., Li, W., Wei, Y., Blanco, M.A., Ren, G., Zhou, T., Storz, P., Wang, H.Y., Kang, Y., 2014. PKD1 phosphorylation-dependent degradation of Snail by SCF-FBXO11 regulates epithelial-mesenchymal transition and metastasis. Cancer Cell 26, 358–373.

Zhang, Y., Young, A., Zhang, J., Chen, X., 2015. P73 tumor suppressor and its targets, p21 and PUMA, are required for madin-darby canine kidney cell morphogenesis by maintaining an appropriate level of epithelial to mesenchymal transition. Oncotarget 6, 13994–14004.

Zhou, B.P., Deng, J., Xia, W., Xu, J., Li, Y.M., Gunduz, M., Hung, M.C., 2004. Dual regulation of Snail by GSK-3beta-mediated phosphorylation in control of epithelial-mesenchymal transition. Nat. Cell Biol. 6, 931–940.

Zhu, L.F., Hu, Y., Yang, C.C., Xu, X.H., Ning, T.Y., Wang, Z.L., Ye, J.H., Liu, L.K., 2012. Snail overexpression induces an epithelial to mesenchymal transition and cancer stem cell-like properties in SCC9 cells. Lab. Invest. 92, 744–752.